Spectrochimica Acta Part A: Molecular and Biomolecular Spectroscopy 191 (2018) 116–124

Contents lists available at ScienceDirect

Spectrochimica Acta Part A: Molecular and Biomolecular Spectroscopy

journal homepage: www.elsevier.com/locate/saa

Unveiling the stimulatory effects of tartrazine on human and bovine serum albumin fibrillogenesis: Spectroscopic and microscopic study

Nasser Abdulatif Al-Shabib [a,*], Javed Masood Khan [a], Mohammad A. Alsenaidy [b], Abdulrahman M. Alsenaidy [c], Mohd Shahnawaz Khan [c], Fohad Mabood Husain [a], Mohammad Rashid Khan [d], Mohammad Naseem [e], Priyankar Sen [f], Parvez Alam [g], Rizwan Hasan Khan [g]

[a] Department of Food Science and Nutrition, Faculty of Food and Agricultural Sciences, King Saud University, 2460, Riyadh 11451, Saudi Arabia
[b] Department of Pharmaceutics, College of Pharmacy, King Saud University, Riyadh, Saudi Arabia
[c] Protein Research Chair, Department of Biochemistry, College of Science, King Saud University, Riyadh 11451, Saudi Arabia
[d] Department of Pharmacology and Toxicology, College of Pharmacy, King Saud University, Riyadh, Saudi Arabia
[e] Electrical Engineering Department, Integral University Lucknow, 226026, India
[f] Centre for Bioseparation Technology, VIT University, Vellore 632014, India
[g] Interdisciplinary Biotechnology Unit, Aligarh Muslim University, Aligarh 202002, India

ARTICLE INFO

Article history:
Received 25 May 2017
Received in revised form 20 August 2017
Accepted 20 September 2017
Available online 22 September 2017

Keywords:
Food additive dye
Tartrazine (TZ)
Amyloid fibril
Protein aggregation
pH
Human and bovine serum albumin

ABSTRACT

Amyloid fibrils are playing key role in the pathogenesis of various neurodegenerative diseases. Generally anionic molecules are known to induce amyloid fibril in several proteins. In this work, we have studied the effect of anionic food additive dye i.e., tartrazine (TZ) on the amyloid fibril formation of human serum albumins (HSA) and bovine serum albumin (BSA) at pHs 7.4 and 3.5. We have employed various biophysical methods like, turbidity measurements, Rayleigh Light Scattering (RLS), Dynamic Light Scattering (DLS), intrinsic fluorescence, Congo red assay, far-UV CD, transmission electron microscopy (TEM) and atomic force microscopy (AFM) to decipher the mechanism of TZ-induce amyloid fibril formation in both the serum albumins at pHs 7.4 and 3.5. The obtained results suggest that both the albumins forms amyloid-like aggregates in the presence of 1.0 to 15.0 mM of TZ at pH 3.5, but no amyloid fibril were seen at pH 7.4. The possible cause of TZ-induced amyloid fibril formation is electrostatic and hydrophobic interaction because sulfate group of TZ may have interacted electrostatically with positively charged amino acids of the albumins at pH 3.5 and increased protein-protein and protein-TZ interactions leading to amyloid fibril formation. The TEM, RLS and DLS results are suggesting that BSA forms bigger size amyloids compared to HSA, may be due to high surface hydrophobicity of BSA.

1. Introduction

Tartrazine (Trisodium 5-hydroxy-1-(4-sulfonatophenyl)-4-(4-sulfonato-phenyl azo)-pyrazole-3-carboxylate); TZ is an anionic orange colored dye (Fig. 1A), highly soluble in water and extensively used in food products, drink, pharmaceuticals and cosmetics [1]. TZ is having N═N linkage with aromatic rings, and hazardous to human health. The maximum acceptable daily intake (ADI) of TZ is recommended to a person is ~7.5 mg/kg body weight [2]. The toxicological concerns of TZ are important and needed high-quality research. Several discrepancies were already found regarding TZ toxicology. In some reports, it has been seen that TZ is showing toxic effects while in other reports TZ is not toxic [3,4]. Recently, it is discovered that low as well as a high concentration of TZ, is altering the function of important biological markers of essential organs such as kidney and liver [5]. It is also known to affect the learning memory functions and reproductive functions of Swiss albino mice [6,7]. The toxicological study of TZ is critical because it is used in a wide verity of food products. In this regard, it will be interesting to see the effect of TZ on proteins structure and function. Earlier, it has been seen that the TZ is altering the secondary structure of human and bovine serum albumin at neutral pH [8].

TZ salt yields four ionic states in solution; H^5L^+ (pH < 3), H^2L^{2-} (pH 3 to 4), HL^{3-} (pH 4 to 6.5) and L^{4-} (pH 7 to10). H^5L^+, H^2L^{2-}, HL^{3-}, L^{4-} exhibited the absorbance maxima at 440 nm, 430 nm, 420 nm and 400 nm respectively. The pKa1 and pKa2 values are 5.15.and 9.25 respectively [9]. Thus, TZ remains in a protonated state at pH 3.5, while deprotonated state at pH 7. TZ has high binding affinity to bovine serum albumin (BSA) compared to human serum albumin (HSA) investigated by isothermal titration calorimetry at pH 7.4 [10]. It has also been found that the small molecules are modulating amyloid

Abbreviations: CR, Congo red; RLS, Rayleigh Light Scattering; DLS, Dynamic Light Scattering; TEM, transmission electron microscopy.

* Corresponding author at: Department of Food Sciences, College of Food and Agricultural Sciences, King Saud University, Riyadh, Saudi Arabia.
E-mail address: nalshabib@ksu.edu.sa (N.A. Al-Shabib).

http://dx.doi.org/10.1016/j.saa.2017.09.062
1386-1425/

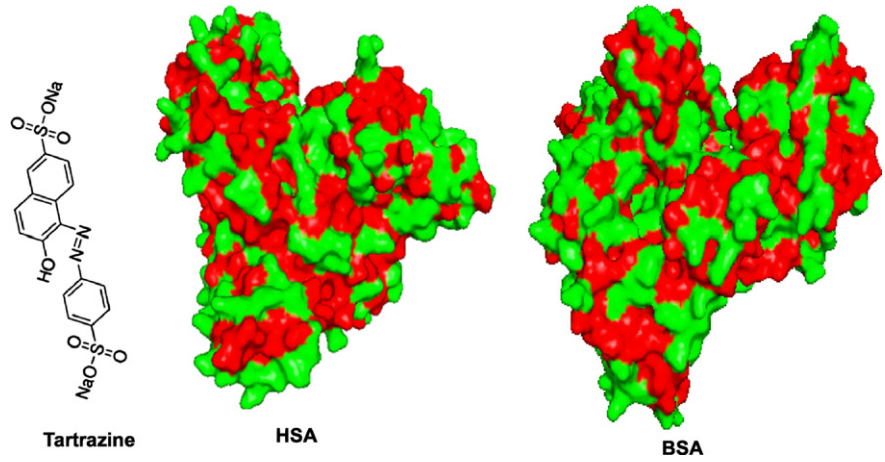

Fig. 1. A: Molecular structure of TZ. Crystal structure of HSA and BSA and hydrophobic amino acids distributions from highlighted in red color.

fibril formation in many proteins at physiological and acidic pH [11,12]. Amyloid fibrils are toxic to the cells and causing various neurodegenerative diseases in humans [13,14]. The amyloid fibrils are a long unbranched polymer of protein monomer; the size of amyloid fibril is found typically 10 nm in diameter to micrometer [15]. Amyloid fibrils are well-organized and insoluble proteins, possessing cross β-sheet structure and showing high ThT dye binding [16]. The mechanism of amyloid fibril formation is still not understood. Several works have been done to find out the mechanism of amyloid fibril formation in proteins under in-vitro condition [17,18].

Serum albumin is a cargo protein, most abundantly found in blood plasma and carried out several physiological functions including transportation and deposition of ligands [19]. HSA and BSA are multifunctional proteins in plasma and share almost 76% sequence homology [20]. They contain two primary ligand binding sites, i.e. Sudlow site I and II. The Sudlow site I, is located in subdomain IIA and site II is located in subdomain IIIA [21]. Tryptophan residues are primary fluorophores in proteins. HSA contains one Trp-residue at 214 positions in subdomain IIA, and BSA contains two Trp-residues at positions 134 and 212. The Trp-134 of BSA was found on the surface of the first domain, and Trp-212 was located in the hydrophobic pocket of the second domain [22]. BSA is relatively more hydrophobic compared to HSA. Total hydrophobic residues on the surface of the serum albumins are highlighted in red color shown in Fig. 1.

Serum albumins are a model protein to study the mechanism of amyloid fibril formation under in-vitro conditions [23,24]. It is reported that HSA and BSA form amyloid fibrils in the presence of three different anionic surfactants at low pH [25].

Previously, we have seen the effect sodium dodecyl sulfate (SDS) on lysozyme at physiological pH and found that SDS is promoting amyloid-like fibril formation [26]. SDS is similar to TZ because both the molecules contain negatively charged sulfate group and hydrophobic chain on the other side. It will be interesting to see the effect of TZ on serum albumin at both physiological as well as low pH conditions. The serum albumins were found in cationic states at low pH and anionic state at neutral pH. It is vastly reported that lots of proteins are found in cationic state under in-vivo conditions so TZ can affect the important function of cationic proteins. In this work, we have studied the effect of a TZ on amyloid induction of two proteins; HSA and BSA, at two specific pHs 3.5 and 7.4. The study also includes the differences of HSA and BSA in amyloid formation with TZ.

2. Experimental

2.1. Materials

Human, Bovine serum albumin, Tris-HCl, TZ and Sodium Acetate were purchased from Sigma Chemicals Co. (St. Louis, MO, USA). All

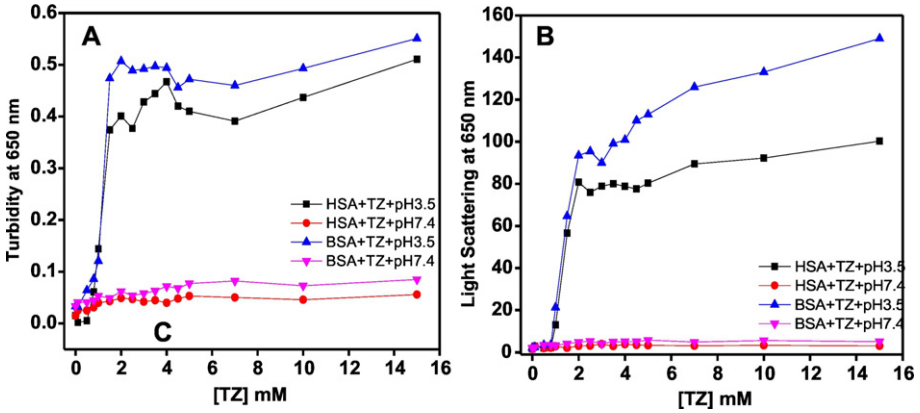

Fig. 2. Turbidity measurements: The effect of increasing concentrations of TZ on human and bovine serum albumin at pH 3.5 (-■-), (-▲-) and 7.4 (-●-), (-▼-) was seen and plotted in panel A. RLS data: Light Scattering at 650 nm of human and bovine serum albumin was plotted with increasing concentrations of TZ at pH 3.5(-■-), (-▲-) and 7.4 (-●-), (-▼-) shown in panel B. The samples were excited at 650 nm and emission was taken at 650 nm. The albumins concentrations were taken 0.2 mg ml^{-1} in both (Turbidity and RLS) the measurements.

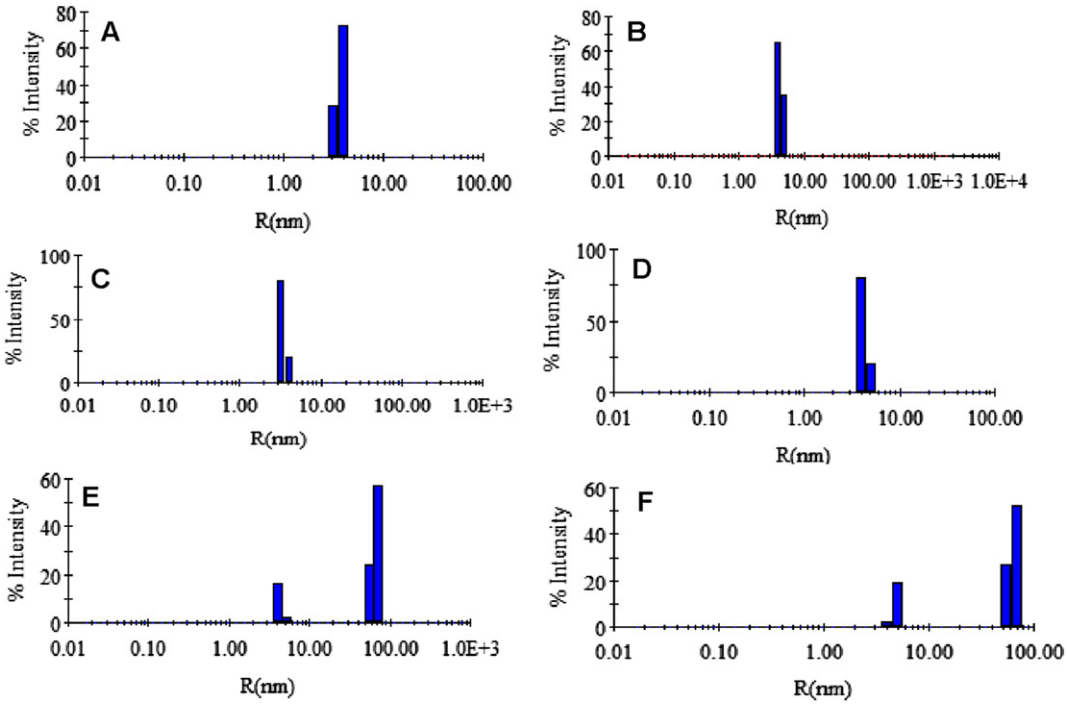

Fig. 3. The hydrodynamic radii of TZ-induced aggregates were measured by DLS: The hydrodynamic radii of human serum albumin at pH 7.4 (A), pH 3.5 (B) and in the presence of 5.0 mM TZ at pH 3.5 (E) are shown. The hydrodynamic radii of BSA at pH 7.4 (C), pH 3.5 (D) and presence of 5.0 mM TZ at pH 3.5 (F). The HSA and BSA concentrations were taken 1.0 mg ml^{-1}.

other reagents and chemicals were used to very high-quality analytical grade. Milli-Q water has been used although for preparing buffers.

2.2. Methods

2.2.1. Stocks of Human and Bovine Serum Albumin Preparation

The human and bovine serum albumin was dissolved in 20 mM, Tris-HCl buffer pH 7.4. The concentrations of human and bovine serum albumins were quantified by taking optical density at 280 nm by a spectrophotometer. The molar absorption coefficient of human and bovine serum albumin was taken at 280 nm is 35,700 and 43,827 M^{-1} cm^{-1} respectively [25].

2.2.2. pH Measurements

The pH of solution, 20 mM of Tris-HCl for pH 7.4 and sodium acetate for pH 3.5 was measured by the Mettler Toledo pH meter. Before experiments, all the buffer solutions were filtered through PVDF 0.25 mm syringe filter from Millipore Milex-HV.

2.2.3. Turbidity Measurements

The turbidity of the solution was measured by Perkin-Elmer double beam UV–Vis spectrophotometer by measuring turbidity at 650 nm. The human and bovine serum albumin concentrations were fixed 0.2 mg ml^{-1} in all the samples. The concentrations of TZ were taken from 0 to 20 mM. The turbidity study was conducted at two different pHs (7.4 and 3.5). Before measurements, all the samples containing human and bovine serum albumin with and without TZ were incubated overnight.

2.2.4. Rayleigh Light Scattering Measurements (RLS)

RLS study was performed to characterize the TZ-induced aggregation in human and bovine serum albumins at two different pHs (7.4 and 3.5). The Jasco FP-750 spectrofluorometer was used to do all the RLS experiments at room temperature with 1.0 cm path length cuvette. Both the albumins were incubated with different concentrations of TZ (0–20 mM) at two different pH, 7.4 and 3.5. Both albumins samples were excited at 650 nm and emission was taken at the same wavelength. The excitation and emission slit widths were set at 5.0 nm in all the measurements. In RLS measurements, we used 0.05 mg ml^{-1} of albumins concentrations at both the pHs because the Light Scattering cannot be measure beyond the value of 1000 a.u.

2.2.5. Dynamic Light Scattering (DLS)

DLS measures the change in hydrodynamic radii of human and bovine serum albumin with response to TZ. The concentrations of serum albumins and TZ were taken 1.0 mg ml^{-1} and 5.0 mM respectively. DLS study was done on a DynaPro-TC-04 Dynamic Light Scattering instrument (Protein Solutions, Wyatt Technology, Santa Barbara, CA) equipped with a temperature-controlled micro-sampler. Every solution was filtered through a Millipore filter with 0.22 μm pore size. The hydrodynamic radii (Rh) and polydispersity (Pd) were calculated by translational diffusion coefficient from the Stokes–Einstein equation [27]:

$$Rh = \frac{kT}{6\pi\eta D}$$

where hydrodynamic radii are denoted as Rh, k is the Boltzmann's constant, T is the absolute temperature (K), η is the viscosity of buffer and D is the translational diffusion coefficient.

Table 1
Hydrodynamic radii (*Rh*) and polydispersity of human and bovine serum albumin incubated at different conditions.

S. no.	Conditions	Hydrodynamic radii (*Rh*) (nm)	Polydispersity (Pd) %
1	HSA at pH 7.4	3.5	12.31
2	BSA at pH 7.4	3.7	10.54
3	HSA at pH 3.5	4.4	16.01
4	BSA at pH 3.5	4.7	18.10
5	HSA at pH 3.5 + 5.0 mM TZ	4.6 and 66.7	40.98
6	BSA at pH 3.5 + 5.0 mM TZ	5.1 and 69.3	42.12

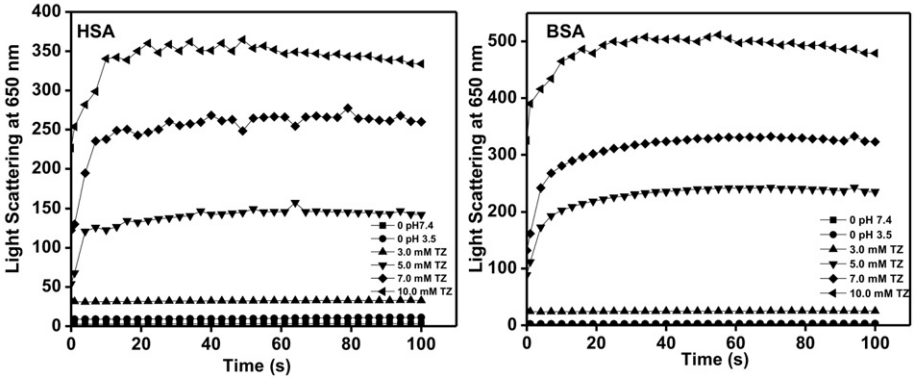

Fig. 4. Kinetics of TZ-induced aggregation: Time evolution of Light Scattering at 650 nm of HSA and BSA in the presence and absence of TZ at pH 3.5 and 7.4. The HSA and BSA concentrations were fixed 0.2 mg ml^{-1} and TZ concentrations were varied.

2.2.6. Time-dependent Kinetics of TZ-induced Aggregation

Kinetics study was carried out on Hitachi F7000 spectrofluorometer at room temperature in the cuvette of 3 ml with 1 cm path length. The serum albumins (HSA and BSA) samples with and without TZ were excited at 650 nm and emission was taken at the 650 nm with respect time in seconds. The excitation and emission slit width were fixed 5 nm and albumin concentrations was taken 0.2 mg ml^{-1} in all the samples. The kinetics study was performed at both pHs (7.4 and 3.5).

2.2.7. Steady-state Fluorescence Measurements

Before steady-state fluorescence study, the TZ-induced-amyloid fibril of serum albumins (HSA and BSA) was centrifuged two times at 5000 RPM for 5 min to remove the excess dye from the samples. The centrifugation and washing was done to nullified the inner filter effects. Jasco FP-750 spectrofluorometer was used to do the intrinsic fluorescence studies of washed samples. An intrinsic fluorescence study was done at room temperature in a 1 cm path length cuvette. In intrinsic fluorescence measurements, the HSA and BSA alone and in the presence of TZ samples were excited at 280 nm and emissions were taken in the range of 300 to 400 nm. The serum albumin concentrations (0.2 mg ml^{-1}) were taken in all the measurements. The excitation and emission slit width were set 5 nm. All the samples were incubated overnight prior intrinsic fluorescence measurements.

2.2.8. Congo Red (CR) Binding

CR dye was dissolved in Milli-Q water and then filtered through 0.2 μ Millipore syringe filter. The concentration of freshly prepared CR was estimated by spectrophotometrically by taking extinction coefficient 45,000 M^{-1} cm^{-1} at 498 nm. TZ-induced aggregated samples were centrifuged two times at 5000 RPM for 5 min to remove the dye. The aggregated and non-aggregated samples were incubated with CR (5.0 μM) for 30 min in the dark. The concentrations of serum albumins were fixed 0.2 mg ml^{-1} and different concentrations of TZ were taken. CR binding study was performed on a Perkin-Elmer double beam UV–Vis spectrophotometer and absorbance was taken in the range of 400–800 nm.

2.2.9. Far-UV CD Measurements

Far-UV CD measured the change in secondary structure of proteins. The Applied Photophysics, Chirascan-Plus, UK spectropolarimeter attached with Peltier and water circulator was used to see the change in secondary structural of serum (HSA and BSA) proteins. Far-UV CD spectra of all the samples were acquired in the range of 200–250 nm. The serum albumins (0.2 mg ml^{-1}) were incubated with different concentrations of TZ for overnight. The incubated samples were centrifuged two times at 5000 RPM for 5 min, and then supernatant was discared and precipitates were redissolve in respective buffer. The centrifugation was done to remove excess dye. Aggregated and non-aggregated samples were scanned three times, and average spectra were taken. The averaged spectra were smoothed by the Savitzky–Golay method.

2.2.10. Transmission Electron Microscopy (TEM)

TEM was performed to identify the morphology of TZ-induced aggregates of serum albumins. JEOL transmission electron microscope operating at an accelerating voltage of 200 kV was used to capture the morphology of aggregates. The 6.0 μl of aggregated samples were taken and applied to on 200-mesh, copper grid covered by the carbon stabilized the formvar film. After a few minutes, the grid was further negatively stained with 2% (w/v) uranyl acetate and leave for dryness.

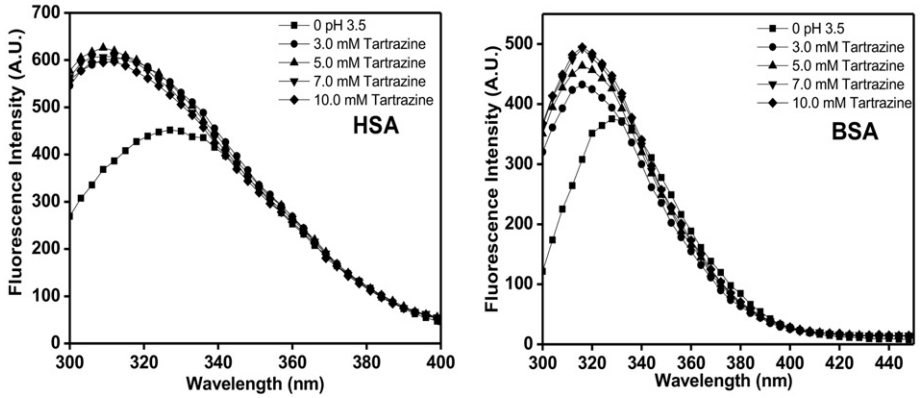

Fig. 5. Intrinsic fluorescence emission spectra of HSA and BSA without TZ (-■-) and with different concentrations of 3.0 mM (-●-), 5.0 mM (-▲-), 7.0 mM (-▼-) and 10.0 mM (-♦-) of TZ. The HSA and BSA concentration was fixed 0.2 mg ml^{-1} in all intrinsic fluorescence measurements.

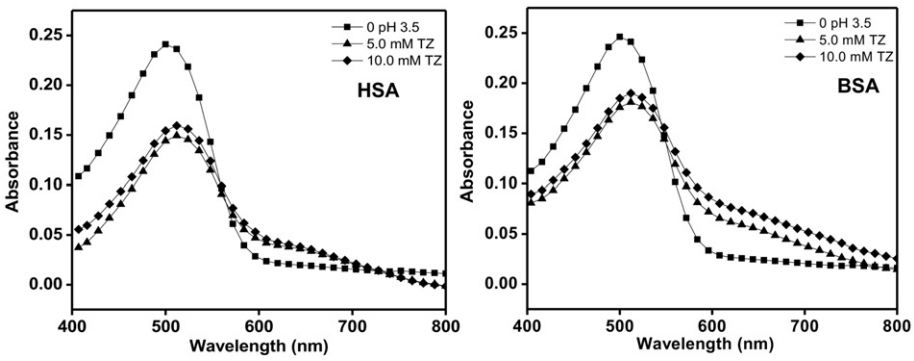

Fig. 6. Absorption spectra of HSA and BSA with Congo red at pH 3.5 (-■-) were plotted and in the presence of different concentrations 5.0 mM (-▲-), and 10.0 mM (-♦-) of TZ. In CR binding measurements albumins and Congo red concentrations were taken 0.2 mg ml^{-1} and 5.0 μM respectively.

The albumin concentrations were fixed 0.2 mg ml^{-1} in all the samples. The images were viewed at high resolution.

2.2.11. Atomic Force Microscopy (AFM)

HSA and BSA (0.2 mg·ml^{-1}) were treated with TZ (5.0 mM) and leave for ~12 h incubation at room temperature in 20 mM sodium acetate buffer, pH 3.5. After incubation 10 μl of the aggregated samples were taken and diluted almost 50 times. Diluted samples were poured on freshly cleaved mica and incubated for 5 min. The mica was rinsed with Milli-Q water and then leaves for one day for dryness. The dried mica was visualized on Bioscope Catalyst AFM (Bruker, USA) in the tapping mode. The captured images were processed for publication by using Nanoscope Analysis v.1.4.

3. Results

3.1. Turbidity at 650 nm Measurements

Turbidity measurements were employed to detect the TZ-induced aggregation in HSA and BSA protein at pH 3.5 and 7.4. The aggregated protein showed high turbidity in the wavelength range of 350–650 nm [28]. The turbidity of the HSA and BSA with and without TZ was measured at pH 3.5 and 7.4 (Fig. 2A). The turbidity was measured at 650 nm because TZ absorbance is almost zero at this wavelength [29]. Below 1.0 mM of TZ, the albumins didn't show any turbidity. However, in the presence of higher concentrations (beyond 1.0 mM) of TZ progressive increase in turbidity was recorded up to 15.0 mM at pH 3.5. However, no turbidity was seen in a sample (HSA and BSA with TZ) at pH 7.4.

3.2. Rayleigh Light Scattering (RLS) Measurements

RLS is a very sensitive spectrofluorimetric technique used to observe the aggregation by scattering at 650 nm. The role of TZ was seen on aggregation of HSA and BSA at two pHs (7.4 and 3.5) shown (Fig. 2B). The scattering profile of HSA and BSA with 1.0 to 15.0 mM TZ showed high scattering at pH 3.5, with higher scattering in the case of BSA and lower in the case of HSA. Albumins with below 1.0 mM TZ couldn't found to induce any scattering at 650 nm. Only base line changes observed in scattering of HSA and BSA with or without TZ at pH 7.4. The turbidity and RLS results suggest that the albumins aggregate in the presence of >1.0 mM TZ at pH 3.5, but no change observes at pH 7.4.

3.3. Dynamic Light Scattering (DLS)

The DLS experiments were carried out to characterize hydrodynamic radii of HSA and BSA with or without 5.0 mM TZ at pH 7.4 and 3.5 respectively, and shown in Fig. 3 and Table 1. It is a known fact that small molecules or ligands can affect the hydrodynamic radii of proteins [30]. The hydrodynamic radii of the HSA and BSA at pH 7.4 were found around 3.5 (Fig. 3A) and 3.7 nm (Fig. 3B) respectively, which is very similar to already published work [31]. However, the hydrodynamic radii and polydispersity of albumins were increased at pH 3.5, from 3.5 nm to 4.1 nm (Fig. 3C) in case of HSA and 3.7 nm to 4.7 nm (Fig. 3D) in case of BSA. This may happen possibly due to partial unfolding of albumins. After incubation with 5.0 mM of TZ, the hydrodynamic radii as well as the polydispersity of HSA (Fig. 3E) and BSA (Fig. 3F) have increased shown in Table 1. The DLS results further confirm that the TZ is inducing bigger size aggregates in the albumins at pH 3.5.

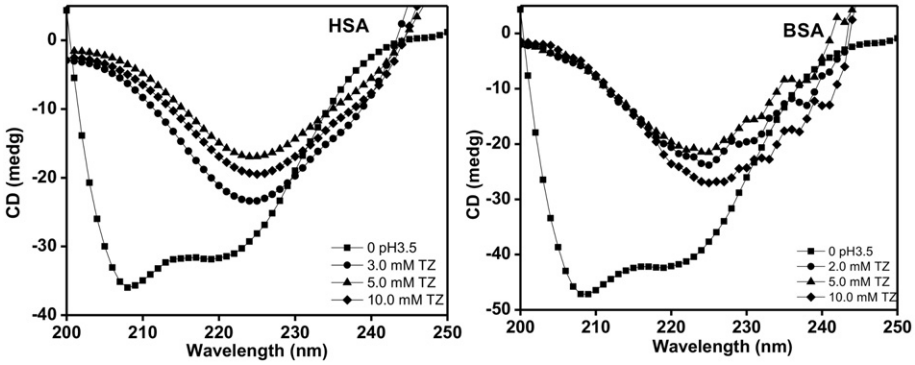

Fig. 7. Far-UV CD spectra of HSA and BSA at pH 3.5 (-■-) and with 2.0 (-●-), 5.0 (-▲-) and 10.0 (-♦-) mM of TZ was plotted in both the figures. Before scanning of CD spectra the aggregated samples were centrifuged and washed with buffers to remove the TZ dye. The centrifugation was done to overcome interference of TZ dye in the far-UV range. The concentration of HSA and BSA was taken constant 0.2 mg ml^{-1} in all the samples.

Table 2
% secondary structure of HSA and BSA without and with different concentration of TZ at pH 3.5 was calculated by K2D2 software.

	HSA				BSA			
	0 pH 3.5	5.0 mM TZ	7.0 mM TZ	10.0 mM TZ	0 pH 3.5	5.0 mM TZ	7.0 mM TZ	10.0 mM TZ
% α-helix	50.16	11.53	11.53	11.53	63.05	13.51	13.51	13.51
% β-sheet	7.14	28.35	28.35	28.35	3.29	31.63	31.63	31.63

3.4. Kinetics of TZ Induced Human and Bovine Serum Albumin Aggregation

We have investigated the effect of different concentrations of TZ on HSA and BSA kinetic fibrillation at pH 3.5 with RLS, by scattering at 650 nm (Fig. 4). The kinetics study was done at six different conditions mentioned in Fig. 4 inset. No change in scattering at 650 nm was observed in the absence of TZ., but in the presence of TZ it was found huge scattering without any lag phase. Irrespective to conditions, TZ-induced aggregation was very fast and saturation achieved within 10 s. Although, intensity of scattering has increased with TZ concentration. Similar kind of rapid kinetics of aggregation has been reported in case of serum albumins and anionic surfactant interaction at low pH [25].

3.5. Intrinsic Fluorescence

We have performed intrinsic fluorescence measurements of albumins in the presence and absence of TZ at pH 3.5 (Fig.5). HSA and BSA in the absence of TZ showed maximum fluorescence intensity (FI) at 335 and 340 nm respectively after excitation at 280 nm. After incubation with different concentrations (3.0, 5.0, 7.0 and 10.0 mM) of TZ, the FI was found to increase with a blue shift in wavelength maximum from 335 to 320 nm in case of HSA and 340 nm to 322 nm in case of BSA. The saturation achieved even at the lowest concentration of TZ (3.0 mM). No further investigation has been done below 3.0 mM of TZ. The blue shift of fluorescence spectra is a sign of the movement of intrinsic fluorophores; like tryptophan, towards more hydrophobic environment. It may have happened due to the formation of intermolecular hydrophobic cluster during aggregation of the albumins [32].

3.6. Congo Red Study

Congo red is a dye used in detection of amyloid fibrils in solutions and tissues. Congo red binds with amyloid fibrils and showing a red-shift in absorbance maximum [33,34]. A Congo red dye binding study was performed with albumins and TZ at pH 3.5, as shown in Fig. 6. In the absence of TZ, albumins show absorbance maximum around 498 nm with Congo red. The absorbance maximum of the HSA and BSA were red-shifted 512 nm and 516 nm respectively, when it was incubated with 5.0 mM TZ at pH 3.5. No further change has been observed in the presence of 5.0 mM TZ. The red-shift in the absorbance maximum of the HSA and BSA in the presence of TZ may happen due to amyloid-like aggregates [35].

3.7. Circular Dichroism Measurements

To gain insight into the secondary structural modifications upon formation of amyloid-like aggregates, we performed far-UV CD experiments. It is vastly reported that any protein whether it contains α, β and random coil as a secondary structure they turn into cross β structure when it form amyloid-like fibrils [36,37]. Far-UV CD spectra of HSA and BSA (Fig. 7) were observed in the absence and presence of TZ at pH 3.5. In the absence of TZ, far-UV CD spectra of human and bovine serum albumins show two minima, one at 208 and another at 222 nm; a unique feature of α-helical proteins [37]. But, in the presence of TZ, a single minima was observed at 225 nm. This resembles the cross β-sheet structure of proteins that shows a single minimum around 225–230 nm [38]. The ellipticity of HSA and BSA spectra was also decreased in the presence of different concentrations of TZ. Similar far-UV CD spectra have been observed in hyperthermophile proteins in the presence of SDS at acidic pH [39]. A change in percent secondary structure of HSA and BSA with response to TZ is shown in Table 2.

3.8. Morphology of TZ-induced Serum Albumins Aggregates

The morphology of TZ-induced aggregates of the HSA and BSA was examined by transmission electron microscopy (TEM). TEM is used to categorize the morphology of aggregates, whether it contains amyloid-like or amorphous aggregates. The shape and size of amyloid fibrils varied depending on the protein and in-vitro factors [40]. TEM images of HSA and BSA in the presence of 5.0 mM TZ at pH 3.5 are shown in Fig. 8. It can be seen from the figure both the proteins (HSA and BSA) are formed amyloid-like aggregates in the presence of TZ. The size of BSA fibrils is found bigger than the size of HSA fibrils. Our all results confirmed that TZ-induced HSA and BSA aggregates show amyloid-like morphology.

3.9. Morphology of TZ-induced HSA and BSA Aggregates Was Evaluated by AFM

The morphology of HSA and BSA aggregates was further analyzed by using atomic force microscopy (AFM) and results are summarizing in Fig. 9A (HSA) and 9B (BSA). HSA and BSA both form long and straight fibril in presence of 5.0 mM TZ at pH 3.5. From the Fig. 9A and B, it was seen that BSA form dense fibril compared to HSA. AFM results is also supported that TZ-induced aggregates have amyloid-like morphology.

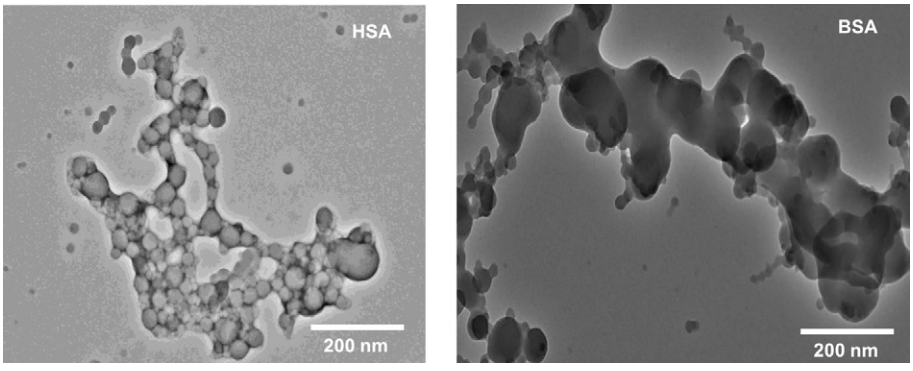

Fig. 8. TEM was done to characterize the morphology of TZ-induced aggregates. The HSA and BSA (0.2 mg ml^{-1}) were incubated with 5.0 mM of TZ at pH 3.5 and sample were leave for overnight incubation at room temperature.

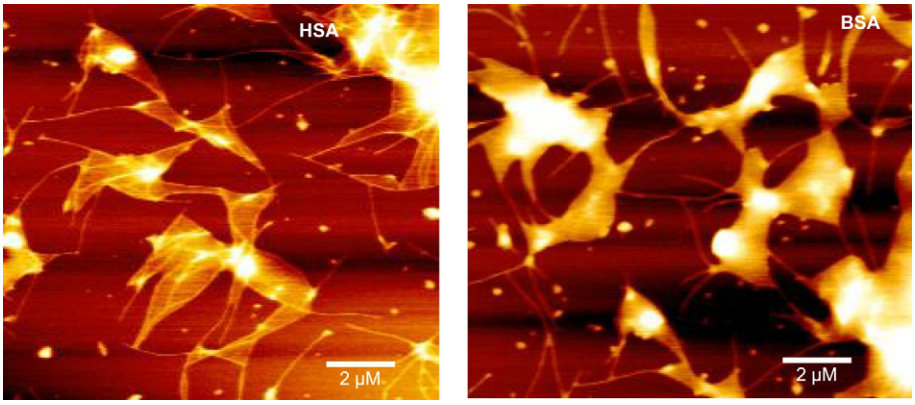

Fig. 9. AFM was carried to characterize the morphology of TZ-induced aggregates. The HSA and BSA (0.2 mg ml^{-1}) were treated with 5.0 mM of TZ at pH 3.5 and TZ treated samples were incubated for overnight at room temperature.

4. Discussion

The anionic molecules are known to promote amyloid fibril formation in many proteins [39,41,42]. However, the mechanisms of amyloid fibril formation by anionic molecules are not clearly understood. Previously, we have reported that the negatively charged surfactant (sodium dodecyl sulfate; SDS) induces amyloid fibril in 25 types of mesophilic proteins via electrostatic and hydrophobic interactions [43]. In this study, our primary goal is to decipher the mechanism of TZ-induced amyloid fibril formation in serum albumins. The isoelectric point (pIs) of human and bovine serum albumins is lying in between 5.67 and 5.65, below this pH both the albumins have a total net positive charge HSA (80.7) and BSA (79.2) as calculated by PROTEIN CALCULATOR v3.3 software [42]. The N state of HSA possesses ~58% alpha helix, while the F state possesses ~46%. The loss of secondary and tertiary structures may be attributed by the loss of domain III of the proteins [44]. F state is partially unfolded that may push some hydrophobic clusters of albumins towards the solvent. The partially unfolded states of proteins are more prone to form amyloid like aggregates [45]. Furthermore, all the selected albumins exhibit a net positive charge at pH 3.5 (pI B 5.5). We have used various biophysical techniques to test the mechanism of TZ-induced aggregation. The Turbidity and RLS results indicate that both the serum albumins become aggregated beyond 1.0 mM of TZ concentrations at pH 3.5. The protonated salt state of TZ (H_2L^{2-}) possesses at least three negatively charged functional groups (two —SO^{3-} and one —COO^{-}) that may act like hooks between protonated amino acid residues of albumins at pH 3.5, and may have formed a salt bridge among the aggregating monomers [9]. This could have given larger accessibility of the solvent accessible hydrophobic moieties of albumins, due to unfolding of domain III, to form inter-molecular hydrophobic interaction that ends in aggregation. In short, both electrostatic and hydrophobic interaction may have played role in TZ-induced aggregation. In contrary, at pH 7.0, the deprotonated and fully folded albumins couldn't be able to interact enough with negatively charged TZ to result in any polymerization.

Turbidity and RLS were also found high due to electrostatic and hydrophobic interaction between lysozyme and SDS below pH 11.0 [46, 26]. The hydrodynamic radii of both the serum albumin were also measured in the absence and presence of TZ at low pH. It has been seen that the hydrodynamic radii of BSA increased at 65 °C and in the presence of 1.0 M, L-Arg at 14 h [47]. In our case, we also found increased in hydrodynamic radii of the HSA and BSA when albumins were exposed to 5.0 mM of TZ at pH 3.5. The hydrodynamic radii results confirmed that TZ binds via ionic interaction with both the serum albumins and

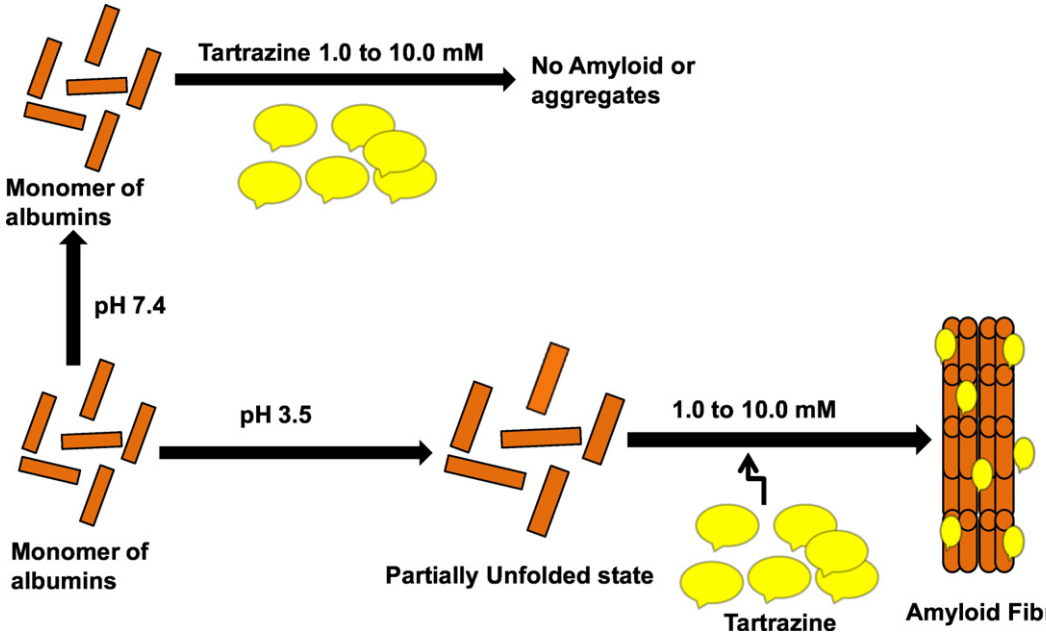

Fig. 10. Diagrammatic presentation of TZ interaction with HSA and BSA at two different pHs (7.4 and 3.5) and mechanism of amyloid fibril formation with TZ.

forming a bigger size aggregates that could be amyloid fibril. Further, we have also seen the kinetics of TZ-induced aggregates in both the albumins at pH 3.5. TZ-induced aggregation is also supported by the fact that seeding of preformed aggregates does not need for the fibrillation process [48]. The RLS was found more in both the albumin when higher concentrations of TZ were added. Similar kind of kinetics was also found when Aβ2M protein was incubated with 0.5 and 1.0 mM of anionic surfactant i.e. SDS, no lag phase was detected, and equilibrium reached after 120 h incubation [49]. Intrinsic fluorescence results also indicate that both the albumins wavelength maximum was found blue shifted in the presence of higher concentrations of TZ. Further, TZ induced aggregate morphology was also detected by Congo red dye binding, TEM and AFM. It has been found that the Congo red has a high affinity to the parallel, antiparallel and cross β-sheet structures of amyloid fibril [50]. Congo red dye binds with TZ-induced aggregates and shift in the absorbance maximum towards higher wavelength. Congo red binding results confirmed that TZ-induced aggregates have amyloid-like aggregates. The TEM and AFM results are also confirmed that TZ-induced aggregates have well organized amyloid-like aggregates. This is good agreement with earlier published reports, the 5.0 mM of negatively charged phospholipid, di hexanoyl phosphatidylserine (DHPS) induced amyloid fibril in apoC-II protein confirmed by TEM [51]. Far-UV CD also monitored the secondary structural level transition. The far-UV CD spectra of both the albumins at pH 3.5, display native-like α-helix. The minima at 208 and 222 nm of both the albumins shifted into single minimum in the range of ~225–230 nm in the presence of various concentrations (2.0, 5.0 and 10.0 mM) of TZ. The minima at 225 and 230 nm is not a characteristic feature of β- sheet protein, but it could be the minima of the cross- β sheet structure. This is widely reported that the amyloid fibril contains cross β-sheet structure. A similar kind of secondary structural minima shift was also noticed in β-sheet protein (Con A) when it was incubated with very low concentrations of cationic surfactant (cetyltrimethylammonium bromide) at physiological pH [52].

4.1. Differences Were Noticed among Human and Bovine Serum Albumin in Response to TZ

Both the serum albumins are similar in structure, but have minute differences in structural stability. The human serum albumin was found thermally more stable compared to bovine serum albumin confirmed by differential scanning calorimetry [53]. Previously, we have also characterized the comparative stability of both serum albumin and found that the BSA is less stable than HSA because BSA contains two tryptophan residues at 134 and 212 position [54]. The charges of the BSA is almost same as the charges of HSA at pH 3.5, but BSA has more surface hydrophobicity compared to HSA [55]. In this study, we found that TZ is inducing bigger size aggregates in BSA compared to HSA, which is confirmed by turbidity, RLS and DLS measurements. The possible cause of larger size aggregate formation in the BSA is surface hydrophobicity not to the net positive charges. It is good agreements with earlier reports; they claimed that protein aromatic residues are playing essential role in amyloid fibril formation [56].

The TZ-induced aggregation and its mechanism of are summarized in Fig. 10. Both the serum albumins contain several positively charged, negatively charged and hydrophobic amino acids. The amino group ($-NH_2$) of all the positively charged amino acids are protonated at pH 3.5 because pI of both the albumins are found around 5.7. It is well established that protein acquires a total net positive charge when it was incubated at pH below two units of the pI and negatively charged residues are uncharged. The negatively charged sulfate group of TZ dye interacted electrostatically with protonated positively charged amino acids and inducing amyloid fibril in both the albumins. However, at pH 7.4, strong electrostatic repulsion was found between both the albumins and negatively charged TZ dye because both the albumins are negatively charged at pH 7.4. Overall our results suggest that the electrostatic and hydrophobic interactions are playing very crucial role in the TZ-induced aggregation process.

5. Conclusion

In this work, our results show that the anionic food additive dye i.e., TZ-induce amyloid-like fibril in HSA and BSA at pH 3.5. The TZ-induced aggregates have a cross β-sheet structure, confirmed by far-UV CD experiments. The TZ is inducing bigger size aggregates in BSA compared to an HSA. These results are indicating that the electrostatic and hydrophobic interactions are key player in the TZ-induced aggregation. Probably, TZ has the potential to induce amyloid fibril in any protein that is positively charged.

Acknowledgements

The authors wish to thanks the Agricultural Research Center, the College of Food and Agricultural Sciences and Deanship of Scientific Research, King Saud University, Saudi Arabia, for supporting this work.

Appendix A. Supplementary data

Supplementary data to this article can be found online at https://doi.org/10.1016/j.saa.2017.09.062.

References

[1] N. Mehdi, S. AinadTabet, N. Mokrane, S. Addou, C. Zaoui, Reproductive toxicology of tartrazine (FD and C Yellow No. 5) in Swiss albino mice, Am. J. Pharmacol. Toxicol. 4 (2009) 128–133.
[2] P. Mpountoukas, A. Pantazaki, E. Kostareli, P. Christodoulou, K. Karelia, S. Poliliou, C. Mourelatos, V. Lambropoulou, T. Lialiaris, Cytogenetic evaluation and DNA interaction studies of the food colorants amaranth, erythrosine and tartrazine, Food Chem. Toxicol. 48 (2010) 2934–2944.
[3] K.J. Davis, O.G. Fitzhugh, A.A. Nelson, Chronic rat and dog toxicity studies on tartrazine, Toxicol. Appl. Pharmacol. 6 (1964) 621–626.
[4] J.F. Borzelleca, J.B. Hallagan, Chronic toxicity/carcinogenicity studies of FD & C Yellow No. 5 (tartrazine) in rats, Food Chem. Toxicol. 26 (1988) 179–187.
[5] K.A. Amin, H.H. Abdel, A.H. Abd-Elsttar, Effect of food azo dyes tartrazine and carmoisine on biochemical parameters related to renal, hepatic function and oxidative stress biomarkers in young male rats, Food Chem. Toxicol. 48 (2010) 2994–2999.
[6] N. Mehedi, S. Ainad-Tabet, N. Mokrane, S. Addou, C. Zaoui, O. Kheroua, D. Saidi, Reproductive toxicology of tartrazine (FD and C yellow No. 5) in Swiss albino mice, Am. J. Pharmacol. Toxicol. 4 (4) (2009) 130–135.
[7] Y. Gao, C. Li, J. Shen, H. Yin, X. An, H. Jin, Effect of food azo dye tartrazine on learning and memory functions in mice and rats, and the possible mechanisms involved, J. Food Sci. 76 (2011) T125–T129.
[8] X. Pan, P. Qin, R. Liu, J. Wang, Characterizing the interaction between tartrazine and two serum albumins by a hybrid spectroscopic approach, J. Agric. Food Chem. 59 (12) (2011) 6650–6656.
[9] M.M.S. Saleh, E.Y. Hashem, N.O.A. Al-Salahi, Oxidation and complexation-based spectrophotometric methods for sensitive determination of tartrazine E102 in some commercial food samples, Comput. Chem. 4 (2016) 51–64.
[10] A. Basu, G.S. Kumar, Thermodynamic of the interaction of the food additive tartrazine with serum albumins: a microcalorimetric investigation, Food Chem. 175 (2015) 137–142.
[11] P.K. Singh, V. Kotia, D. Ghosh, G.M. Mohite, A. Kumar, S.K. Maji, Curcumin modulates α-synuclein aggregation and toxicity, ACS Chem. Neurosci. 4 (3) (2013) 393–407.
[12] J.M. Khan, M.S. Khan, A. Qadeer, M.A. Alsenaidy, A. Ahmed, N.A. Al-Shabib, R.H. Khan, Cationic gemini surfactant (16-4-16) interact electrostatically with anionic plant lectin and facilitates amyloid fibril formation at neutral pH, Colloids Surf. A Physicochem. Eng. Asp. 522 (2017) 494–502.
[13] R.A. Smith, A. Nabok, B.J. Blakeman, W.F. Xue, B. Abell, D.P. Smith, Analysis of toxic amyloid fibril interactions at natively derived membranes by ellipsometry, PLoS One 10 (7) (2015), e0132309. .
[14] M. Ahmed, J. Davis, D. Aucoin, T. Sato, S. Ahuja, S. Aimoto, J.I. Elliott, W.E. Van Nostrand, S.O. Smith, Structural conversion of neurotoxic amyloid-beta (1-42) oligomers to fibrils, Nat. Struct. Mol. Biol. 17 (5) (2010) 561–567.
[15] M. Stefani, Biochemical and biophysical features of both oligomer/fibril and cell membrane in amyloid cytotoxicity, FEBS J. 277 (22) (2010) 4602–4613.
[16] T. Sneideris, D. Darguzis, A. Botyriute, M. Grigaliunas, R. Winter, V. Smirnovas, pH-driven polymorphism of insulin amyloid-like fibrils, PLoS One 10 (8) (2015), e0136602. .
[17] K.E. Kumar, D.K. Prasad, P.N. Prabhu, Concentration dependent switch in the kinetic pathway of lysozyme fibrillation: spectroscopic and microscopic analysis, Spectrochim. Acta A Mol. Biomol. Spectrosc. 183 (2017) 187–194.

[18] A.P. Chaudhary, N.H. Vispute, V.K. Shukla, B. Ahmad, A comparative study of fibrillation kinetics of two homologous proteins under identical solution condition, Biochimie 132 (2017) 75–84.
[19] J. Ghuman, P.A. Zunszain, I. Petitpas, A.A. Bhattacharya, M. Otagiri, S. Curry, Structural basis of the drug-binding specificity of human serum albumin, J. Mol. Biol. 353 (2005) 38–52.
[20] B.X. Huang, H.Y. Kim, C. Dass, Probing three-dimensional structure of bovine serum albumin by chemical cross-linking and mass spectrometry, J. Am. Soc. Mass Spectrom. 15 (2004) 1237–1247.
[21] M. Hossain, A.Y. Khan, S.G. Kumar, Interaction of the anticancer plant alkaloid sanguinarine with bovine serum albumin, PLoS One 6 (2011), e18333. .
[22] P. Banerjee, S. Ghosh, A. Sarkar, S.C. Bhattacharya, Fluorescence resonance energy transfer: a promising tool for investigation of the interaction between 1-anthracene sulphonate and serum albumins, J. Lumin. 131 (2011) 316–321.
[23] J. Juárez, P. Taboada, V. Mosquera, Existence of different structural intermediates on the fibrillation pathway of human serum albumin, Biophys. J. 96 (6) (2009) 2353–2370.
[24] L.L. Zhang, F.F. Ma, Y.F. Kuang, S. Cheng, Y.F. Long, Q.G. Xiao, Highly sensitive detection of bovine serum albumin based on the aggregation of triangular silver nanoplates, Spectrochim. Acta A Mol. Biomol. Spectrosc. 154 (2016) 98–102.
[25] J.M. Khan, S.A. Abdulrehman, F.K. Zaidi, S. Gourinath, R.H. Khan, Hydrophobicity alone cannot trigger aggregation in protonated mammalian serum albumins, Phys. Chem. Chem. Phys. 16 (11) (2014) 5150–5161.
[26] J.M. Khan, S.K. Chaturvedi, S.K. Rahman, M. Ishtikhar, A. Qadeer, E. Ahmad, R.H. Khan, Protonation favors aggregation of lysozyme with SDS, Soft Matter 10 (15) (2014) 2591–2599.
[27] J.T. Edward, Molecular volumes and the Stokes-Einstein equation, J. Chem. Educ. 47 (1970) 261.
[28] Y. Kawachi, R. Kameyama, A. Handa, N. Takahashi, N. Tanaka, Role of the N-terminal amphiphilic region of ovalbumin during heat-induced aggregation and gelation, J. Agric. Food Chem. 61 (36) (2013) 8668–8675.
[29] O. Sha, X. Zhu, Y. Feng, W. Ma, Determination of sunset yellow and tartrazine in food samples by combining ionic liquid-basedaqueous two-phase system with high performance liquid chromatography, J. Anal. Methods Chem. 2014 (2014) 964273.
[30] S.K. Chaturvedi, J.M. Khan, M.K. Siddiqi, P. Alam, R.H. Khan, Comparative insight into surfactants mediated amyloidogenesis of lysozyme, Int. J. Biol. Macromol. 83 (2016) 315–325.
[31] S.K. Chaturvedi, M.K. Siddiqi, P. Alam, M. Zamana, R.H. Khan, Comparative binding study of anti-tuberculosis drug pyrazinamide with serum albumins, RSC Adv. 6 (2016) 85860–85869.
[32] A. Qadeer, E. Ahmad, M. Zaman, M.W. Khan, J.M. Khan, G. Rabbani, K.F. Tarique, G. Sharma, S. Gourinath, S. Nadeem, G. Badr, R.H. Khan, Concentration-dependent antagonistic persuasion of SDS and naphthalene derivatives on the fibrillation of stem bromelain, Arch. Biochem. Biophys. 540 (2013) 101–116.
[33] J.M. Wang, X.Q. Yang, S.W. Yin, D.B. Yuan, N. Xia, J.R. Qi, Growth kinetics of amyloid-like fibrils derived from individual subunits of soy β-conglycinin, J. Agric. Food Chem. 59 (20) (2011) 11270–11277.
[34] W.E. Klunk, R.F. Jacob, R.P. Mason, Quantifying amyloid by Congo red spectral shift assay, Methods Enzymol. 309 (1999) 285–305.
[35] W.E. Klunk, Quantitative evaluation of Congo red binding to amyloid-like proteins with a beta-pleated sheet conformation, J. Histochem. Cytochem. 37 (1989) 1273–1281.
[36] J.W. Wu, K.N. Liu, S.C. How, W.A. Chen, C.M. Lai, H.S. Liu, C.J. Hu, S.S. Wang, Carnosine's effect on amyloid fibril formation and induced cytotoxicity of lysozyme, PLoS One 8 (12) (2013), e81982. .
[37] M.F. Symmons, S.G. Buchanan, D.T. Clarke, G. Jones, N.J. Gay, X-ray diffraction and far-UV CD studies of filaments formed by a leucine-rich repeat peptide: structural similarity to the amyloid fibrils of prions and Alzheimer's disease beta-protein, FEBS Lett. 412 (2) (1997) 397–403.
[38] P. Sen, S. Fatima, J.M. Khan, R.H. Khan, How methyl cyanide induces aggregation in all-alpha proteins: a case study in four albumins, Int. J. Biol. Macromol. 44 (2) (2009) 163–169.
[39] J.M. Khan, P. Sharma, K. Arora, N. Kishor, P. Kaila, P. Guptasarma, The Achilles' heel of "ultrastable" hyperthermophile proteins: submillimolar concentrations of SDS stimulate rapid conformational change, aggregation, and amyloid formation in proteins carrying overall positive charge, Biochemistry 55 (28) (2016) 3920–3936.
[40] H.A. Lashuel, S.R. Labrenz, L. Woo, L.C. Serpell, J.W. Kelly, Protofilaments, filaments, ribbons, and fibrils from peptidomimetic self-assembly: implications for amyloid fibril formation and materials science, J. Am. Chem. Soc. 122 (22) (2000) 5262–5277.
[41] D. Sambasivam, S. Sivanesan, B.S. Ashok, J. Rajadas, Structural preferences of Aβ fragments in different micellar environments, Neuropeptides 45 (6) (2011) 369–376.
[42] E. Hellstrand, A. Nowacka, D. Topgaard, S. Linse, E. Sparr, Membrane lipid co-aggregation with α-synuclein fibrils, PLoS One 8 (10) (2013), e77235. .
[43] J.M. Khan, A. Qadeer, S.K. Chaturvedi, E. Ahmad, S.A. Rehman, S. Gourinath, R.H. Khan, SDS can be utilized as an amyloid inducer: a case study on diverse proteins, PLoS One 7 (1) (2012), e29694. .
[44] B. Ahmad, S. Parveen, R.H. Khan, Effect of albumin conformation on the binding of ciprofloxacin to human serum albumin: a novel approach directly assigning binding site, Biomacromolecules 7 (4) (2006) 1350–1356.
[45] V.N. Uversky, A.L. Fink, Conformational constraints for amyloid fibrillation: the importance of being unfolded, Biochim. Biophys. Acta 1698 (2) (2004) 131–153.
[46] A.A. Moosavi-Movahedi, P. Pirzadeh, S. Hashemnia, S. Ahmadian, B. Hemmateenejad, M. Amani, A.A. Saboury, F. Ahmad, M. Shamsipur, G.H. Hakimelahi, F.Y. Tsai, H.H. Alijanvand, R. Yousefi, Fibril formation of lysozyme upon interaction with sodium dodecyl sulfate at pH 9.2, Colloids Surf. B: Biointerfaces 60 (1) (2007) 55–61.
[47] K.N. Liu, H.Y. Wang, C.Y. Chen, S.S. Wang, L-Arginine reduces thioflavin T fluorescence but not fibrillation of bovine serum albumin, Amino Acids 39 (3) (2010) 821–829.
[48] N.K. Holm, S.K. Jespersen, L.V. Thomassen, T.Y. Wolff, P. Sehgal, L.A. Thomsen, G. Christiansen, C.B. Andersen, A.D. Knudsen, D.E. Otzen, Aggregation and fibrillation of bovine serum albumin, Biochim. Biophys. Acta 1774 (9) (2007) 1128–1138.
[49] S. Yamamoto, K. Hasegawa, I. Yamaguchi, S. Tsutsumi, J. Kardos, Y. Goto, F. Gejyo, H. Naiki, Low concentrations of sodium dodecyl sulfate induce the extension of beta 2-lmicroglobulin-related amyloid fibrils at a neutral pH, Biochemistry 43 (34) (2004) 11075–11082.
[50] C. Wu, J. Scott, J.E. Shea, Binding of Congo red to amyloid protofibrils of the Alzheimer Aβ(9-40) peptide probed by molecular dynamics simulations, Biophys. J. 103 (3) (2012) 550–557.
[51] T.M. Ryan, G.J. Howlett, M.F. Bailey, Fluorescence detection of a lipid-induced tetrameric intermediate in amyloid fibril formation by apolipoprotein C-II, J. Biol. Chem. 283 (50) (2008) 3518–3528.
[52] J.M. Khan, M.S. Khan, M.S. Ali, N.A. Al-Shabib, R.H. Khan, Cetyltrimethylammonium bromide (CTAB) promote amyloid fibril formation in carbohydrate binding protein (concanavalin A) at physiological pH, RSC Adv. 6 (2016) 38100–38111.
[53] A. Michnik, K. Michalik, A. Kluczewska, Z. Drzazga, Comparative DSC study of human and bovine serum albumin, J. Therm. Anal. Calorim. 84 (2006) 113–117.
[54] E. Ahmad, P. Sen, R.H. Khan, Structural stability as a probe for molecular evolution of homologous albumins studied by spectroscopyand bioinformatics, Cell Biochem. Biophys. 61 (2) (2011) 313–325.
[55] G. Tubio, B. Nerli, G. Picó, Relationship between the protein surface hydrophobicity and its partitioning behaviour in aqueous two-phase systems of polyethyleneglycol-dextran, J. Chromatogr. B Anal. Technol. Biomed. Life Sci. 799 (2) (2004) 293–301.
[56] E. Gazit, A possible role for pi-stacking in the self-assembly of amyloid fibrils, FASEB J. 16 (1) (2002) 77–83.